Mon. Not. R. astr. Soc. (1984) **210**, 79–88

Gravitational lens model of the double QSO 0957 + 561 A, B incorporating *VLBI* features

D. Narasimha*, K. Subramanian and S. M. Chitre
Tata Institute of Fundamental Research, Homi Bhabha Road, Bombay 400 005, India

Accepted 1984 February 7. Received 1983 November 22; in original form 1983 August 30

Summary. The twin quasar QSO 0957 + 561 A, B along with bright radio arches and *VLBI* structures is modelled using a gravitational lens consisting of the giant elliptical galaxy and the background cluster. The effective time-delay between components A and B comes out to be around one yr, which is significantly different from the value obtained by Young *et al.* for similar set of lens parameters. It is demonstrated that the observed intensity variation in component B between 1979 and mid-1981, reported by Keel (1982) can result from minilensing by low mass stars.

1 Introduction

The twin quasar Q0957 + 561 A, B is generally believed to be a single object whose light has been split into two or more images by gravitational lensing. Detailed lens models have been constructed by Young *et al.* (1981) which include the combined gravitational effects of an elliptical galaxy and a background cluster at $z = 0.36$. These reproduce satisfactorily the observed separation of 6.15 arcsec and intensity ratio of 1.3 between the components A, B. (Walsh, Carswell & Weymann 1979). Porcas *et al.* (1981) report the *VLBI* observations of the twin quasar which have revealed the core-jet type structures with extensions of 46 ± 1 milliarcsec and 56 ± 2 milliarcsec respectively for the components A, B and the respective position angles of $21° \pm 1°$ and $17° \pm 1°$. Any attempt to model the double quasar must take into account these *VLBI* features.

The *VLBI* core-jet structures will clearly restrict the admissible lens models and we demonstrate that it is possible to model the core-jet extensions and position angles in the framework of a gravitational lens consisting of the giant elliptical galaxy and the surrounding cluster. The observational data, however, is still not adequate to define the lens model uniquely, and what is particularly needed is the position of the effective cluster-centre.

2 Gravitational lens model

2.1 MATHEMATICAL FORMULATION

We follow the notation of Young *et al.* (1981) and first reproduce their results before proceeding to image the *VLBI* features. For this purpose we use the complex formalism developed by Bourassa & Kantowski (1975), and define a complex function $I(x_0, y_0)$

* Present address: Department of Physics, University of Calgary, Canada T2N 1N4.

called the scattering function which incorporates all the information we need about the lens properties. The source and image positions, projected onto the plane of the deflector and described by the complex numbers $Z = X + iY$ and $Z_0 = X_0 + iY_0$ respectively, are related by the equation

$$Z = Z_0 - \frac{4GD_{ds}D_d}{c^2 D_s} I^*(X_0, Y_0), \tag{1}$$

where D_d, D_s and D_{ds} are the deflector, source and deflector-source angular distances respectively in a Robertson-Walker universe. Throughout we have adopted a cosmological model with $q_0 = 0$ and $H_0 = 60$ km s^{-1} Mpc^{-1}. For the purpose of our computations we have taken into account the combined gravitational influence of the elliptical galaxy and cluster (Young *et al.* 1981). We assume the galaxy and the smooth cluster mass distributions to be described by a density profile of the form $(r_c^2 + r^2)^{-3/2}$ (r_c, core radius). For the cluster, we also include the effect of individual galaxies in the cluster within 50 arcsec of the quasar. However, we find their effect to be insignificant if we follow Young *et al.* (1981) by taking one solar mass of galaxy matter to have a red magnitude, R, of 50 and the cluster centre located ~ 23 arcsec west of the galaxy. The scattering function can be written as

$$I(X_0, Y_0) = M_g \frac{\exp(-i\theta_g)}{r_c} f\left(\frac{\exp(i\theta_g)}{r_c} Z_0\right) + M_{cl} \frac{\exp(-i\theta_{cl})}{R_{cl}} f\left[\frac{\exp(i\theta_{cl})}{R_{cl}} (Z_0 - u)\right]$$
$$+ \sum_i M_i/(Z_0 - Z_i). \tag{2}$$

We have chosen the centre of the galaxy as the origin and the x- and y-coordinates as the right ascension and declination respectively (*cf.* Young *et al.* 1981). Here M_g, M_{cl} are the galactic and cluster masses; r_c, R_{cl} their core-radii; θ_g, θ_{cl} the position angles of their major axes, u the position of the cluster centre, M_i the masses of the individual galaxies in the cluster, Z_i their positions and the function f is as derived in Narasimha, Subramanian & Chitre (1982). Defining the line-of-sight velocity dispersion as in Young *et al.* (1981) by

$$\sigma^2 = 4\pi G \rho_0 a^2, \tag{3}$$

where ρ_0 is the central density and a the structural length given by $r_c/3$, expressing Z_0 and Z in arcsec units and using equation (2), we get,

$$Z = Z_0 - \frac{36D_{ds}}{D_s}\left(\frac{\sigma_g}{c}\right)^2 (1 - e_g^2)^{1/2}\, \delta_g \exp(i\theta_g) f^*\left[Z_0 \exp(i\theta_g) \frac{D_d}{r_c}\right]$$
$$- \frac{36D_{ds}}{D_s}\left(\frac{\sigma_{cl}}{c}\right)^2 (1 - e_{cl}^2)^{1/2}\, \delta_{cl} \exp(i\theta_{cl}) f^*\left[\exp(i\theta_{cl}) \frac{D_d}{R_{cl}} (Z_0 - u)\right]$$
$$- \sum_i 4GM_i D_{ds}/c^2 D_s D_d (Z_0 - Z_i)^*. \tag{4}$$

Here e_g, e_{cl} are the eccentricities of the galaxy and cluster mass distributions and $\delta = \ln[(n^2+1)^{1/2} + n] - n/(n^2+1)^{1/2}$, where n is the ratio of the cut off radius to the core radius defined by $\rho(r) = 0$ for $r/r_c \geqslant n$.

2.2 NUMERICAL RESULTS

Our aim is to locate the images by finding the roots of equations (4) for a given source position Z. Once the image positions are known, we can find their amplifications by varying the source positions in equation (4) over a small region and finding the corresponding variation in the image position. Further the time-delays can be obtained using the

expressions given by Cooke & Kantowski (1975). In order to model the observed quasar configuration we adopt the following procedure.

We prescribe the core-radii, ellipticities, major axis position angles of the lens galaxy and the background cluster and also specify the position of image A and its associated core-jet structure. For a given choice of the right ascension of the cluster centre with respect to the lens galaxy, we then fit the position and intensity of image B along with its core-jet to conform with observations. In practice we are able to achieve this by varying the velocity dispersion of the galaxy and of the cluster and the declination of the cluster centre, until the desired configuration and the *VLBI* structure associated with image B are reasonably reproduced. In Table 1(a) we summarize such solutions for the range of right ascensions of the cluster centre (−19 to −35 arcsec) suggested by Young *et al.* (1981) corresponding to the following choice of lens parameters.

	core-radius	cut-off radius	eccentricity	PA of major axis
galaxy:	3 kpc	60.0 kpc	0.6	37°
cluster:	170 kpc	1.7 Mpc	0.8	25°

The typical separation between components A and B is ~ 6.2 arcsec and the effective time-delay between the images, $t_B - t_A$ comes out to be 1−1.4 yr with intensity variation of image A preceding that of image B.

It should be emphasized at this stage that the imaging of *VLBI* structures does impose stringent constraints on possible lens models. In fact, for a given right ascension of the cluster centre and for the parameters of the galaxy and cluster quoted above, we find the observed *VLBI* image configuration to be reproduced only for a very small spread of the velocity dispersion of the galaxy and the cluster (to within a few km s^{-1}) and for a reasonably narrow range of the declination of the cluster centre (0.1 arcsec). Further, the image configuration in which the axes of the core-jets are aligned almost parallel is obtained only for a rather narrow range of source positions lying close to the critical curve across

Table 1. (a) Solutions for a range of right ascensions of the cluster centre (−19 to −35 arcsec) with density profile $(r^2 + r_c^2)^{-3/2}$.

	Position of Cluster centre wrt galaxy (arcsec) RA	Dec.	σ_g km s^{-1}	σ_{cl} km s^{-1}	Intensity ratio I_A/I_B	Separation AB (arcsec)	Core-jet (B) Extension (milli-arcsec)	Position angle	Time delay (yr) ($t_B - t_A$) Geom.	Potential	Total
(a)	−19	−4.6	269	914	1.36	6.14	54	17.3°	−0.97	2.01	1.04
(b)	−23	−6.9	288	925	1.46	6.14	54	17.2°	−1.70	2.91	1.21
(c)	−27	−8.7	300	946	1.47	6.15	54	15.5°	−2.05	3.38	1.33
(d)	−31	−10.25	303	987	1.49	6.14	54	17.4°	−2.39	3.75	1.36
(e)	−35	−11	306	1027	1.45	6.13	55	16.9°	−2.59	3.99	1.40

(b) Imaging details of case

	Source position (arcsec) RA	Dec.	Image position (arcsec) RA	Dec.	Amplification	Intensity ratio
A			−1.368	5.057	3.330	B1/A = 1.46
B1	−9.295	−0.922	−0.274	−0.987	−2.277	B2/A = 0.14
B2			−0.056	−0.416	0.464	
C	−5.265	1.405	4.23	7.40	2.727	
D	−7.187	0.674	1.60	7.06	2.957	
E	−12.218	−2.322	−5.73	2.06	5.569	

which a transition from one to three images region occurs. It is therefore encouraging to note that the model incorporating the *VLBI* observations naturally requires the large scale radio arch to be modelled only once around image A, with hardly any trace of it around B, a feature that is borne out by VLA observations.

The imaging details of the quasar components A, B1 and B2 are given in Table 1(b). We also give the source positions corresponding to the lobes C, D and E. Evidently, an almost linear structure around the source can be modelled to produce the bright arched bridge extending from component A in the north-eastern direction with its near-absence around B. Notice that the lens parameters can be so arranged that the second image B1 is about 70 per cent as bright as image A, while the third image B2 which is typically 0.5 arcsec from B1 comes out to be about 2 mag fainter. It turns out that in our lens models the imaging of the *VLBI* core-jet features invariably leads to the intensity of the third B2 image about 10 per cent of that of A with a faint core-jet at B2 which is some 30 milliarcsec long and at a position angle of $-155°$. Such an image configuration results provided we restrict ourselves to the effective position of the cluster-centre, 19–30 arcsec west of G1, suggested by Young *et al.* (1981). However, if we relax this condition and move the cluster-centre closer to G1, it does become possible to dim the B2 image with its intensity a few per cent of that of A.

The recent observational limits on the intensity of the third image are quite stringent. The *VLBI* observations of Gorenstein *et al.* (1983) and Gorenstein (1983) agree in the main with the earlier results of Porcas *et al.* (1981). Further Gorenstein *et al.* (1983) and Gorenstein (1983) report a compact component close to the galaxy-centre which is about 2.6 per cent of that of A, while the optical observations of Stockton (1980) give an upper limit for intensity of B2 roughly 1.5 per cent of that of image A. The recent VLA observations by Roberts *et al.* (1983) point to an intensity of B2 image, approximately 2–3 per cent of A. Clearly, in view of these observations it is desirable to explore lens models which not only explain the *VLBI* core-jet features, but also satisfy the constraints on the intensity of the third image. To this end we first analyze the expressions for the amplification in some detail to enquire what must be done to bring down the intensity of the third image.

The amplification $\mathscr{L}$ of an image situated at Z_0 is given by (*cf.* Bourassa & Kantowski 1975)

$$\mathscr{L} = \frac{1}{E^2 - |F|^2}, \tag{5}$$

where E is a real function given by

$$E = 1 - \frac{4\pi G D_{ds} D_d}{c^2 D_s}\sigma \tag{6}$$

and

$$F = \frac{2GD_{ds}D_d}{c^2 D_s}\left[\frac{\partial I}{\partial X_0} - i\frac{\partial I}{\partial Y_0}\right] \tag{7}$$

is a complex quantity. Here σ is the projected surface mass density of the deflector and I is the scattering function defined in Section 2. Notice that E is completely determined by the 'local' value of the surface density, whereas F depends on the value of the surface density at points other than the image position. Furthermore, in the regions far from the lens where the surface density becomes negligible, $E \to 1$ and $|F| \to 0$, and $\mathscr{L} \to 1$. In fact, in

any lens configuration there is always one image, for which $\mathscr{L}$ in equation (5) is positive, and which survives complete misalignment of the source. With progressive alignment of the source and the lens extra images appear in pairs [since any smooth distribution always produces an odd number of images, see Burke (1981)], with opposite phases, that is opposite signs for $\mathscr{L}$. We shall refer to these extra images as 'internal' images. In our lens models B1 and B2 are the internal images, with $\mathscr{L}$ having positive sign for B2 and negative sign for B1. This implies $|E| > |F|$ for the B2 image. Clearly, in order to produce a small value for the intensity of the B2 image, one must have a large value for $|E|$, or a large value for the surface density at the position of the B2 image. This can be achieved either by (1) having a kink in the surface density at the position of the B2 image, or (2) by increasing the central surface density of the galaxy. Note that B2 is closest (~ 0.16 arcsec) to the centre of the galaxy.

The central surface density σ_0 is related to the velocity dispersion σ_g', and core radius, r_c by $\sigma_g^2 \propto \sigma_0 r_c$. Consequently, it is possible to increase the central surface density by either increasing the velocity dispersion or by decreasing the core radius, r_c. [That the intensity of B2 can be decreased by decreasing r_c was also noted by Young *et al.* (1981) on the basis of their numerical computations.] The possibility of increasing the velocity dispersion of the galaxy is ruled out basically since for the large value of σ_g implied ($\gtrsim 400$ km s^{-1}), it becomes extremely difficult to model the *VLBI* feature. This is because, for large σ_g the gravitational effect of the cluster has to be decreased to maintain a separation of ~ 6 arcsec between the components A and B and this means that we no longer have an effective galaxy–cluster asymmetry which can be used to adjust the *VLBI* core-jet features to the observed values. Further for a small value of the galactic core-radius r_c, σ and hence E falls of sufficiently rapidly away from the centre of galaxy, so as to make $E^2 \sim |F|^2$ at the position of B1 image, thereby increasing the intensity of B1 and reducing $\mathscr{L}_{B2}/\mathscr{L}_{B1}$ for these models.

We have therefore attempted lens models with smaller values of the core-radius $r_c \sim 1$ kpc. We are able to construct models which not only reproduce the *VLBI* features satisfactorily but which also have a faint B2 image with intensity less than a few per cent of that of B1 image. However, we find that the cluster centre has to be moved outside the range suggested by Young *et al.* (1981) 19–30 arcsec west of G1, and brought closer to the galaxy centre. We summarize the imaging details of a typical solution in Table 2.

Even though the third image B2 can be considerably dimmed by bringing the cluster centre close to the galaxy, it turns out that the cluster has a very strong influence on the nearby features. The radio lobe E, for example, is then on the verge of being multiply imagined. In all our solutions, we have taken this fact into account and have ensured that there is only one image of E formed as a result of lensing. However, we feel that other scenarios to dim the third image, without relaxing the cluster centre position, such as the 'kink' in the surface mass density σ, mentioned earlier, should also be explored in the future. Clearly, what is particularly needed is a measurement of the position of the effective cluster centre.

In order to test the sensitivity of our results to changes in the density distribution, we have also examined lens models using the density distribution given by Young *et al.* (1981). Here also a satisfactory solution could be obtained after bringing the cluster centre close (~ 6 arcsec) to the galaxy centre. The imaging details of a sample solution obtained in this case are summarized in Table 3. This solution is similar to the one obtained by Harding *et al.* (in Walsh 1983).

In all of our models two features are worthy of note. All the lens models imply a linear magnification by a factor ~ 2–3. It is tempting to speculate that further *VLBI* observations

Table 2. (a) Model lens parameters. Density profile $\rho\alpha(r^2 + r_c^2)^{-3/2}$.

	Galaxy	Cluster
Centre	(0, 0) arcsec	(−2.4, −6.404) arcsec
Core-radius	1.57 kpc	184 kpc
Velocity dispersion	237.5 km s^{-1}	1036.5 km s^{-1}
Eccentricity	0.6	0.85
Position angle of major axis	42°	13.4°
		R = 47.0 mag $M_\odot^{-1}$

(b) Imaging details

	Source position (arcsec) RA	Dec.	Image position (arcsec) RA	Dec.	Amplification	Intensity ratio
A			−1.368	5.057	5.553	
B1	−0.730	−5.249	−0.197	−1.009	−4.436	B1/A = 1.25
B2			−0.004	−0.199	0.141	B2/A = 0.025
C	2.101	−3.667	4.230	7.40	4.685	
D	0.770	−4.135	1.60	7.06	4.648	
E	−2.843	−6.197	−5.73	2.06	9.115	

		Extension (milliarcsec)	Position angle (deg)
Core-jets	A	50	21
	B1	50	13
	B2	11	−159.1

Time delay ($t_B - t_A$) = 0.9545 yr
Separation between A and B = 6.18 arcsec

of this object may reveal the existence of apparent superluminal motion of components of order ~3c. The calculated effective (geometrical + potential) time-delay given in Tables 1, 2 and 3 indicates that image A should show intensity variation ahead of B by 0.7–1.4 yr. Young *et al.* (1981) report the corresponding value of 3–6 yr from their calculations for the time-delay. Our results for time-delay are in general agreement with those given by Dyer & Roeder (1981), and we believe the variance of our calculated time-delay from that of Young *et al.* is because of a sign error in their potential time-delay expression.

3 Effect of minilensing

The intensity of the twin quasar Q0957 + 561 A, B has been monitored since its discovery in the spring of 1979. Until the middle of 1981, component A did not seem to show any sensible flux variation, while the intensity of component B, which was about 70 per cent of that of A in the beginning, showed a rapid brightening to an intensity slightly above A by 1980 October and has since declined gradually (Miller, Antoucci & Keel 1981; Keel 1982; Gott 1983).

Now such a behaviour is difficult to account for on the basis of intrinsic variation in the quasar, if the component A varies in intensity ahead of B by only a yr or so, as predicted by our calculation of the time-delay. For in such a situation, A would also have shown intensity variation during its monitoring between end 79 and mid 81. We have therefore examined the possibility of the intensity variation of the B image resulting from the operation of minilensing by low mass stars (Gott 1981).

Table 3. (a) Model lens parameters. Density distribution of Young *et al.* (1981).

	Galaxy	Cluster
Centre	(0, 0) arcsec	(−2.7, −7.0) arcsec
Core-radius	1.00 kpc	180 kpc
Velocity dispersion	244.5 km s^{-1}	990 km s^{-1}
Eccentricity	0.6	0.85
Position angle of major axis	42°	12°
		R = 48.0 mag $M_{\odot}^{-1}$

(b) Imaging details

	Source position (arcsec) RA	Dec.	Image position (arcsec) RA	Dec.	Amplification	Intensity ratio
A			−1.368	5.057	5.574	B1/A = 1.22
B1	−0.788	−5.363	−0.198	−0.999	−4.563	B2/A = 0.007
B2			−0.003	−0.113	0.039	
C	1.904	−3.735	4.23	7.40	4.428	
D	0.617	−4.217	1.60	7.06	4.495	
E	−2.781	−6.261	−5.73	2.06	8.662	

		Extension (milliarcsec)	Position angle (deg)
Core-jets	A	50	21
	B1	54	17
	B2	5.5	−160.9

Time delay $(t_B - t_A)$ = 0.6453 yr
Separation between A and B = 6.17 arcsec

Recently Schild & Weekes (1983) have monitored the CCD brightness of the twin quasar to find an increase in the B/A intensity ratio of ≈ 0.27 mag during the first half of 1980, followed by a decline towards the end of 1980. According to these authors this behaviour is in satisfactory agreement with the results obtained by Keel from a photographic monitoring of the quasar. Schild & Weekes also report random intensity variations of A and B images by ≈ 0.1 mag. Since observationally the difference in the magnitudes of images (i.e. the ratio B/A of intensities) is a better determined quantity than the individual magnitudes of images (Keel 1982) and noting that Keel's observations had an error ≈ 0.09 mag per plate, the observations of Schild & Weekes also seem to suggest the operation of minilensing in the B image during the period between the end of 1979 and the middle of 1981. Schild & Weekes (1983) have also reported the brightening of the northern image (A) by ≈ 0.15 mag between 1982 May and November. Our model calculations indicate that an intrinsic quasar variation should first manifest in A and later in B with a time-lag of several months to a yr. It will be interesting to see whether the B image shows a corresponding brightening during the latter half of 1983 or the beginning of 1984.

For the purpose of examining the viability of minilensing we have done detailed numerical computations to determine the nature of intensity fluctuations of image B, as a star in the lens galaxy (G1) passes in front of it. In particular we examine whether we can reproduce the light-curve observed by Keel (1982). It may be pointed out that the problem considered here is somewhat different from the one treated by Chang & Refsdal (1979). They take the star to be a member of a spherical lens galaxy, whereas we have a combination of an elliptical galaxy and a cluster acting as a lens for the double quasar. We take the trajectory of the star, $Z_s(t)$, to be a straight line passing close to B at an impact parameter

distance b, and tilted at an angle ϕ to the x-axis. (This is a reasonable approximation to the actual stellar trajectory, since the scales we are interested in $\approx 10^{-6}$ arcsec, are very much smaller than the scales over which stellar trajectories will show significant curvature.)

We add the stellar scattering function to the left-hand side of equation (4) and use the fact that the source position in equation (4) is to be kept fixed when we add the star to the lens model to get

$$0 = \left.\frac{\partial Z}{\partial x_0}\right|_{Z_{0B}} R_e(Z_{0S} - Z_{0B}) + \left.\frac{\partial Z}{\partial y_0}\right|_{Z_{0B}} I_m(Z_{0S} - Z_{0B}) - 4GM_s D_{ds}/c^2 D_d D_s (Z_{0S} - Z_s)^*. \quad (8)$$

Here M_s is the mass of the star, Z_{0B} is the position of image B prior to minilensing and Z_{0s}'s are the positions of the new images which appear as a result of minilensing. We have also used the fact that on the angular scales of the splitting of image B due to the star (namely, 10^{-6} arcsec) the galaxy and cluster scattering functions which will vary only on the arcsec scale, can be linearized. For each fixed Z_s, the roots of equation (8) give the location of the new images due to the star. The image intensities can be computed by varying Z over a small region as before. Since present day techniques are unable to resolve these extra images into individual components (with a separation of $\approx 10^{-6}$ arcsec) we add their individual intensities to get the net amplification of image B due to minilensing. In Fig. 1 we show a plot of the variation in the intensity ratio, B/A as the lens star moves along a trajectory inclined at an angle $\phi \approx \pi/3$ to the x-axis, for three values of the impact parameter $\alpha = 1.20$, $\beta = 1.35$, $\gamma = 1.5$. The lens parameters adopted for this purpose are those corresponding to the solution displayed in Table 2. Note that the impact parameter has been expressed in units of an effective radius of influence $r_0 = (4GM_s D_{ds} D_d/c^2 D_s)^{1/2}$. The observed light curve given by Keel (1982) is also shown in Fig. 1. We have computed similar plots for other values of ϕ, but the choice of $\phi \simeq \pi/3$, seems to be in better accord with the observations. In order to compare the calculated plots with the observed light curve, we should convert the distances along the star path (expressed in units of the critical radius r_0), to the time-scale unit of 'yr'. This can be achieved once the mass and velocity of the lensing star are known, by simply using the relation $v\Delta t = xr_0$. Here v is the transverse velocity of the lensing star, and x the distance traversed by the star in units of r_0. The computed light curve is fitted to the observed light curve given by Keel (1982) by varying the parameter r_0/v. A comparison of the observations given by Keel (1982) with the curves shown in Fig. 1, indicates that a value of b between $1.3r_0$ and $1.4r_0$ (for $\phi = \pi/3$), reproduces satisfactorily both the initial rapid brightening of image B and the subsequent slow fading of its intensity, provided we adopt a value for the combination $(M_s/1\,M_\odot)^{1/2}$ $(1000\ \mathrm{km\ s^{-1}\ V^{-1}}) \sim 0.05$. If we assume a value for the transverse velocity V of the star $\approx 300\ \mathrm{km\ s^{-1}}$ the mass of the star turns out to be $\approx 2.25 \times 10^{-4}\,M_\odot$. However, if V is taken to be the transverse velocity of G1 through the cluster $\approx 1000\ \mathrm{km\ s^{-1}}$ (Canizares 1982), the value of M_s would then become $\approx 2.5 \times 10^{-3}\,M_\odot$. The minilensing by stars in this mass range may marginally affect an inhomogeneous broad line emitting region (Gilmore 1981). However, these stars are not expected to affect the radio emission if it arises from regions $\gtrsim 10^{17}$ cm.

Finally, it is perhaps worthwhile clarifying some points raised by Young (1981) in the context of minilensing. Young (1981) has examined the effect of minilensing by stars to suggest a lower limit of ~ 0.02 pc to the source-size from consideration of the observed intensity variation being less than 30 per cent. This lower limit is arrived at by appealing to the argument that if the source-size were much smaller, then the lensing star would cause much larger intensity variation than what is observed. Young uses this source-size to

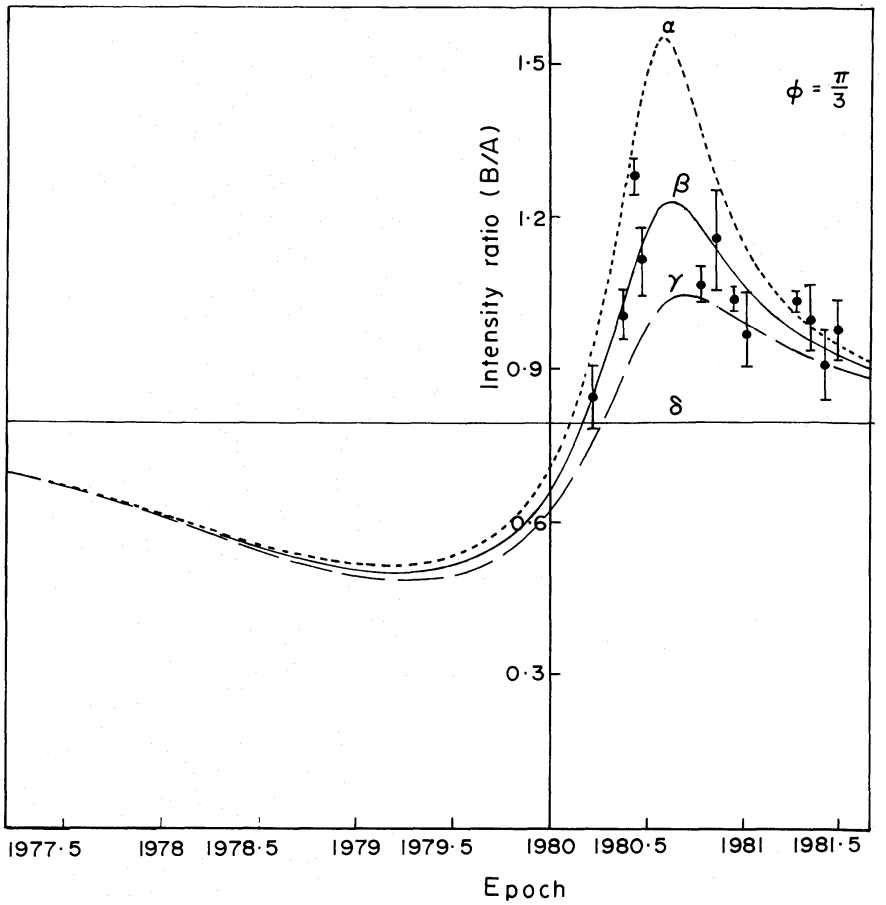

Figure 1. Light curve of Q0957+561 B is displayed as intensity ratio (B/A) for a lensing star moving along the direction $\phi = \pi/3$ as a function of epoch for three values of the impact parameter $\alpha = 1.5$, $\beta = 1.3$ and $\gamma = 1.2$. The line δ corresponds to the intensity ratio prior to minilensing. The observed points with error bars given by Keel (1982) are indicated by filled circles.

calculate the number of low-mass stars ($\approx 10^{-2}\,M_{\odot}$) which come in the beam to be of order 72 and concludes that the effect of such a large number of stars on the beam would wash out any intensity variation in the images. However, it should be pointed out that the maximum amplification due to a lensing star can be decreased not only by enlarging the source-size, but also by having a finite impact parameter for the passage of individual stars close to the image. Thus, even for a point source, low amplitude perturbations in intensity can result on account of lensing stars with a finite impact parameter. Clearly, it is not possible to set a lower limit to the source-size using the observed variation of ≈ 30 per cent in intensity. In this context the number of stars which affect an image is determined by the critical radius of influence of the star, namely, r_0 and not by the number within the arbitrary source-size of 0.02 pc inferred from the intensity variation. And, as pointed out by Gott (1981) the number of stars which can then influence any image is independent of the mass of the lensing star and depends only on the lens parameters and the image-position in relation to the centre of the galaxy. Gott (1981) estimates the expected number of stars to be ≈ 2 for the B image and 0.6 for the A image.

4 Conclusions

From our calculations the following conclusions emerge:

(1) It is possible to incorporate the *VLBI* features of the double quasar Q0957+561 A, B in the framework of a gravitational lens model.

(2) The modelling of the *VLBI* features restricts the range of parameters for the lens galaxy and the cluster and also naturally requires the large scale jet to be imaged only once around image A with its near-absence around B. The observational information is, however, still not adequate for defining a unique model. To achieve this, it will be desirable to know the position of the cluster-centre.

(3) The effective (geometrical + potential) time-delay comes out to be 0.7–1.4 yr (i.e. A varies in intensity ahead of B by 0.7–1.4 yr) (with $H_0 = 60$). This time-delay does not seem to be too sensitive to the choice of lens parameters needed to explain the observations.

(4) The calculated time-delay of several months to about one year and the observed intensity variation in image B can be explained as arising due to minilensing by a low mass star ($2 \times 10^{-4} - 2 \times 10^{-3}\ M_\odot$). Any intrinsic variation in the quasar should be reflected first in component A and should be observed in B several months to a year later.

Acknowledgments

It is a pleasure to thank Richard Porcas and Richard Gott for valuable discussions and helpful comments. We would like to express our gratitude to Drs D. Walsh, D. Roberts and M. V. Gorenstein for sending us their pre-prints. Thanks are also due to a referee whose comments have led to an improvement in the earlier version of the manuscript.

References

Bourassa, R. R. & Kantowski, R., 1975. *Astrophys. J.*, **195**, 13.
Burke, W. L., 1981. *Astrophys. J.*, **244,** L1.
Canizares, C. R., 1982. *Astrophys. J.*, **263,** 508.
Chang, K. & Refsdal, S., 1979. *Nature,* **282,** 561.
Cooke, J. M. & Kantowski, R., 1975. *Astrophys. J.*, **195,** L11.
Dyer, C. C. & Roeder, R. C., 1980. *Astrophys. J.*, **241,** L133.
Gilmore, G., 1981. *Observatory,* **101,** 170.
Gorenstein, M. V., Shapiro, I. I., Cohen, N. L., Corey, B. E., Falco, E. E., Marcaide, J. M., Rogers, A. E. E., Whitney, A. R., Porcas, R. W., Preston, R. A. & Ruis, A., 1983. *Science,* **219,** 54.
Gorenstein, M. V., 1983. *Proc. 24 Liege Int. Astrophys. Colloquium on Quasars and Gravitational Lenses* (Université de Liège), ed. Swings, J.-P.
Gott, J. R., 1981. *Astrophys. J.*, **243,** L135.
Gott, J. R., 1983. *Am. Sci.*, **71,** 150.
Keel, W. C., 1982. *Astrophys. J.*, **255,** 20.
Miller, J. S., Antoucci, R. R. J. & Keel, W. C., 1981. *Nature,* **289,** 153.
Narasimha, D., Subramanian, K. & Chitre, S. M., 1982. *Mon. Not. R. astr. Soc.*, **200,** 941.
Porcas, R. W., Booth, R. S., Browne, I. W. A. & Wilkinson, P. N., 1981. *Nature,* **289,** 758.
Roberts, D. H., Greenfield, P. E., Hewitt, J. N., Burke, B. F. & Dupree, A. K., 1983. Preprint.
Schild, R. E. & Weeks, T., 1983. Center for Astrophysics Preprint No. 1790.
Stockton, A., 1980. *Astrophys. J.*, **242,** L141.
Walsh, D., Carswell, R. F. & Weymann, R. J., 1979. *Nature,* **279,** 381.
Walsh, D., 1983. *Proc. 24 Liege Int. Astrophys. Colloquium on Quasars and Gravitational Lenses* (Université de Liège), ed. Swings, J.-P.
Young, P., Gunn, J. E., Kristian, J., Oke, J. B. & Westphal, J. A., 1981. *Astrophys. J.*, **244,** 736.
Young, P., 1981. *Astrophys. J.*, **244,** 756.